JPE 18-6-20

https://doi.org/10.6113/JPE.2018.18.6.1830
ISSN(Print): 1598-2092 / ISSN(Online): 2093-4718

Modelling and Performance Analysis of UPQC with Digital Kalman Control Algorithm under Unbalanced Distorted Source Voltage conditions

Venkatesh Kumar† and Rajeswari Ramachandran*

†Dept. of Electrical and Electronic Eng, Karunya Institute of Technology and Science, Coimbatore, India
*Dept. of Electrical and Electronic Eng., Government College of Technology, Coimbatore, India

Abstract

In this paper, the generation of a reference current and voltage signal based on a Kalman filter is offered for a 3-phase 4wire UPQC (Unified Power Quality Conditioner). The performance of the UPQC is improved with source voltages that are distorted due to harmonic components. Despite harmonic and frequency variations, the Kalman filter is capable enough to determine the amplitude and the phase angle of load currents and source voltages. The calculation of the first state is sufficient to identify the fundamental components of the current, voltage and angle. Therefore, the Kalman state estimator is fast and simple. A Kalman based control strategy is proposed and implemented for a UPQC in a distribution system. The performance of the proposed control strategy is assessed for all possible source conditions with varying nonlinear and linear loads. The functioning of the proposed control algorithm with a UPQC is scrutinized and validated through simulations employing MATLAB/Simulink software. Using a FPGA SPATRAN 3A DSP board, the proposed algorithm is developed and implemented. A small-scale laboratory prototype is built to verify the simulation results. The stated control scheme for the UPQC reduces the following issues, voltage sags, voltage swells, harmonic distortions (voltage and current), unbalanced supply voltage and unbalanced power factor under dynamic and steady-state operating conditions.

Key words: Active power filter, Distortions, Imbalance voltage, Kalman filter, Phase locked loop (PLL), Synchronous reference frame (SRF), Unified power quality conditioner (UPQC)

I. INTRODUCTION

Recently, industries in the utility sector have been utilizing power converters made up of semi-conductors to achieve better performance in terms of energy conservation and increased production. Although power electronic converters are used extensively in industries, they have certain short comings such as a poor power factor, harmonics, non-sinusoidal supply voltage, reactive burden and low system efficiency. The main objectives of this paper are to mitigate these problems and ensure that power is delivered with acceptable, marginal variations that meet stringent power quality standards [1]-[3].

UPQC is a device that can be used to compensate voltage and current related problems such as voltage imbalance and current harmonics. Its composition includes a series and parallel active power filter (APF). UPQC is highly sought after in the industrial distribution power systems since it is a readily accepted as a device to improve the overall power quality [4]-[6].

The concept of a UPQC in power quality improvement is highly dependent on its speed and precise output with which its control strategies work. In particular, this controller has two algorithms, namely an algorithm for the generation of reference current and one for the generation of reference voltage control. The latter, which operates in a controller, shows accurate and efficient extraction of both current and voltage harmonics [7], [8].

A large number of algorithm studies can be found in the literature such as Synchronous Reference Frame, DQ Theory with Fourier (DQF), Instantaneous Power (PQ) Theory, Fast Fourier Transform (FFT), Synchronous Detection (SD), Wavelet-Based Approach, Artificial Neural Network (ANN) and several others [9]-[12].

Manuscript received Sep. 29, 2017; accepted May 31, 2018
Recommended for publication by Associate Editor Kyo-Beum Lee.
†Corresponding Author: venkateshkumar@karunya.edu
Tel: +91-9597138321, Fax: +91-422-2615615, Karunya Inst. Technol. Sci.
*Dept. Electr. Electron. Eng., Government College of Technology, India

Amongst these algorithms, the SRF algorithm has an edge over others in terms of performance, due in large part to its simple design, increased speed and small number of calculations, which makes it preferable for practical implementation [13]. The main disadvantage of the SRF method is its need for a decisive Phase Locked loop technique which cannot achieve its function in distorted or unbalanced supply voltages. To overcome this disadvantage, several investigations have been carried out by tuning the field of the PLL with different methods. However, the synchronization of the phase angle failed during real time operation of the hardware prototype model [14], [15].

The problems mentioned were addressed through a signal processing-based control algorithm to generate a reference current plus voltage. To develop the routine and scrutiny of non-stationary signals either such as short Fourier transforms, Kalman filtering with others. A Fast Fourier Transforms (FFT) is used to extract distortions of load currents and source voltages. In a steady-state condition, the accuracy of the response to this algorithm is generally accepted. However, the estimates change in the amplitude of the fundamental component requires a delay of at least one cycle [21], [22].

The Kalman Filter is used to estimate and identify the harmonics of the grid and to support harmonic evaluations during dynamic conditions. Most studies have proposed the above method for evaluation instead of implementation. Upon implementation in any power quality conditioner, the algorithm becomes complex and its performance becomes sluggish.

In order to minimize the complexity of a UPQC, the gains of the controller and Kalman filters are calculated offline and then implemented online as constant gains. This is not supported for highly distorted and transient states, which leads to losses in system performance in real time [16].

In addition, during system modeling, its error values are taken into consideration, which adversely affects the performance of the system [17]. Due to changes in the system parameters, the error associated with it changes, and the system performance is further affected [16], [17]. This has been implemented for single phase system and not three phase system.

In [18], system modeling that involves d-q transformations increases the complexity of the system and degrades the response time of the system. In [16]-[18], the time regulation for the stabilization of DC link voltage is not given a lot of importance and is not discussed for various stages during the operation of the system. In addition, the phase angle is also not mentioned, which is necessary for the synchronization of PQ devices with a distribution system.

This paper proposes a Kalman filter based UPQC under variable operating conditions and it is found to be very flexible. The fundamental components of the current, voltage and angle can be obtained from the 1st state itself. As a result, this method is fast and simple. The Kalman filter does not require a PLL and any transformation method. The time taken for the stabilization of the dc-link voltage through this concept, when compared with a PLL with a SRF, an enhanced PLL with a SRF [19] and a resistive optimization technique with a UVT [20], is found to be less than 0.01 seconds. The proposed method ensures that the THD of the source current and load voltage is well below 2% when compared to the above-mentioned techniques. Thus, a unity power factor is maintained under all dynamic load conditions. This is the most versatile technique for the generation of reference compensation signals under unbalanced and distorted supply conditions.

The proposed control algorithm has been implemented with a low-cost single Xilinx Spartan 3A DSP-XC3SD1800 under steady-state and dynamic conditions. The results illustrate the practicality of the proposed control algorithm which is flexible for different operating conditions. The total harmonic distortion (THD) in the source current and load voltage is significantly reduced to meet IEEE 519 and IEC EN 61000-3 standards, which compensate reactive power for non-linear loads.

Section II describes the system configuration of the UPQC. In Section III, the Kalman filter estimation technique is derived and reviewed. In Section IV, the proposed Kalman filter based UPQC is discussed in detail. Sections V and VI presents simulation and experimental results under different operating conditions. Section VII concludes the paper with a discussion of its future scope and validation.

II. UPQC-System Configuration

The combined configuration of a shunt and series power active filter is shown in Fig. 1, which aids in the reimbursement of the voltage and current in an instantaneous way. This configuration has the ability to compensate imbalances of power supplies with harmonic content and harmonic currents of non-linear loads. The outcome of the configured UPQC shows an improvement in power quality.

The configured UPQC consist of dual pulse width modulation converters, which are connected back to back by means of a common DC link. It also accommodates an integrated controller, to set up for the voltage and current of the pulse width modulation converters.

III. Power Quality- State Estimation Technique

The proposed Kalman filter estimator by an LS algorithm expeditiously extricates the magnitude and phase angle of distorted signals, which includes load current and source voltage [23]-[27].

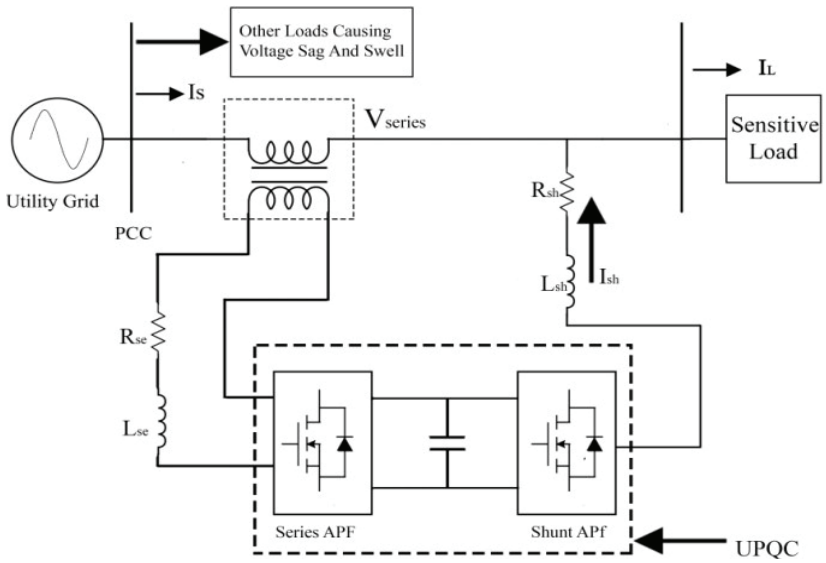

Fig. 1. Schematic diagram of a UPQC.

A. Describing a Signal with Harmonics

During the initial stage of the analysis, the fundamental component of the signal is handled. After that, harmonic components are injected. Thus, mathematical model is formulated that represents the grid voltage dynamics.

The Output voltage of a grid connected system is represented by Eq. (1):

$$signal\ (S_k) = M_k \sin(\omega_k t_k + \theta_k) \tag{1}$$

where:

M_k - Amplitude of the signal

ω_k - Angular frequency

θ_k- Phase Angle of the signal

Signals in terms of Cartesian coordinates are given in Eq. (2) and Eq. (3).

$$x_1(k) = M_k \sin(\omega_k t_k + \theta_k) \tag{2}$$

$$x_2(k) = M_k \cos(\omega_k t_k + \theta_k) \tag{3}$$

Initially, consider:

$$\begin{aligned} M_{k+1} &= M_k\ , \omega_{k+1} \cong \omega_k \& \theta_{k+1} \\ &\cong \theta_k\ at\ the\ time\ t_{k+1} = t_k + T_s \\ S_{k+1} &= M_{k+1} \sin(\omega_k t_k + \omega_k T_s + \theta_{k+1}) \end{aligned}$$

$$\begin{aligned} x_1(k+1) &= M_k \sin(\omega_k t_k + \theta_{k+1} + \ \omega_k T_s) \\ &= M_k[\sin(\omega_k t_k + \theta_k)\cos(\omega_k T_s) \\ &\quad + \cos(\omega_k t_k + \theta_k)\sin(\omega_k T_s)] \\ &= x_1(k)\cos(\omega_k T_s) + x_2(k)\sin(\omega_k T_s) \end{aligned} \tag{4}$$

$$\begin{aligned} x_2(k+1) &= M_k \cos(\omega_k t_k + \theta_{k+1} + \omega_k T_s) \\ &= M_k\,[\cos(\omega_k t_k + \theta_k)\cos(\omega_k T_s) \\ &\quad - \sin(\omega_k t_k + \theta_k)\sin(\omega_k T_s)] \\ &= x_2(k)\cos(\omega_k T_s) - x_1(\mathrm{k})\sin(\omega_k T_s)] \end{aligned} \tag{5}$$

For the modelling amplitude (or) phase variations in a signal, a perturbation vector $[W_1\ W_2]_k^T$ in the system states is considered.

A stochastic state space model for grid connected systems is given in Eq. (6).

$$\left.\begin{aligned} \dot{x} &= Ax + BU + W \\ y &= Cx + DU + V \end{aligned}\right\} \tag{6}$$

The state -space representation of the signal then becomes:

$$\begin{bmatrix} x_1 \\ x_2 \end{bmatrix}_{(k+1)} = \begin{bmatrix} \cos(\omega_k T_s) & \sin(\omega_k T_s) \\ -\sin(\omega_k T_s) & \cos(\omega_k T_s) \end{bmatrix} \begin{bmatrix} x_1 \\ x_2 \end{bmatrix}_{(k)} + \begin{bmatrix} W_1 \\ W_2 \end{bmatrix}_{(k)} \tag{7}$$

$$y_k = [1\ \ 0] \begin{bmatrix} x_1 \\ x_2 \end{bmatrix}_{(k+1)} + V_k \tag{8}$$

Where V_k represents the measurement noise.

If there are n frequencies in the signal S_k:

$$S_k = \sum_{i=1}^{n} M_{ik} \sin(i\omega_k t_k + \theta_{ik}) \tag{9}$$

The state space representation of the signal becomes:

$$\begin{bmatrix} x_1 \\ x_2 \\ . \\ . \\ . \\ x_{2(n-1)} \\ x_{2n} \end{bmatrix}_{(k+1)} = \begin{bmatrix} M_1 & \cdots & 0 \\ \vdots & \ddots & \vdots \\ 0 & \cdots & M_n \end{bmatrix} \begin{bmatrix} x_1 \\ x_2 \\ . \\ . \\ . \\ x_{2(n-1)} \\ x_{2n} \end{bmatrix}_{(k)} + \begin{bmatrix} W_1 \\ W_2 \\ . \\ . \\ . \\ W_{2(n-1)} \\ W_{2n} \end{bmatrix}_{(k)} \tag{10}$$

$$y_k = [1\ \ 0\ \ \cdots\ \ 1\ 0] \begin{bmatrix} x_1 \\ x_2 \\ . \\ . \\ . \\ x_{2(n-1)} \\ x_{2n} \end{bmatrix}_{(k)} + V_k \tag{11}$$

$$M_i = \begin{bmatrix} \cos(i\omega_k T_s) & \sin(i\omega_k T_s) \\ -\sin(i\omega_k T_s) & \cos(i\omega_k T_s) \end{bmatrix}$$

$$\text{So, } A = \begin{bmatrix} M_1 & \cdots & 0 \\ \vdots & \ddots & \vdots \\ 0 & \cdots & M_n \end{bmatrix} \quad C = [1\ 0\ \cdots\ 1\ 0]$$

B. The Kalman Filter (Kf) Algorithm

A set of mathematical equations is employed in the Kalman filter to develop a recursive method to estimate a state in order to minimize the mean square error.

Recursive Kalman filter loop:

The Kalman state vector $X_{(K+1)}$ at any instant can be calculated as follows:

$$X_{(K+1)} = AX_{(K)} + BU_{(k)} + W$$

$$Y_{(k)} = CX_{(K)} + V$$

Where,

$X_{(K+1)}$ -State vector,

A -Transition matrix,

B - Input control vector,

W- Process noise (assumed to be white Gaussian noise with a zero mean and covariance matrix Q),

$Y_{(k)}$ - Observation of the state $X_{(K+1)}$,

C - Observation matrix,

V - Observation noise, (also assumed to be Gaussian white noise with a zero mean and R covariance matrix).

The Kalman filter calculations are two stages in the prediction and updating stages. In the prediction stage, the state is predicted based on the previous instant until recent data is measured. Later the calculations are fed into the updating stage to modify the prediction.

Let us choose an initial state estimate x (0), R as measurement noise covariance and Q as process noise covariance, as the initial state covariance mainly based on intuition.

For the prediction stage

State prediction:

$$X_{K+1/k} = AX_{K/k} + BU_k \tag{12}$$

Measurement prediction:

$$Y_{K+1/k} = CX_{K+1/k} \tag{13}$$

State prediction covariance:

$$P_{(K+1)/k} = AP_{K/k}A^T + Q \tag{14}$$

Measurement prediction covariance:

$$S_{K+1/k} = CP_{K+1/k}C^T + R \tag{15}$$

For the updating stage

Kalman filter gain:

$$G_{K+1} = P_{K+1/k}C^T[S_{K+1/k}]^{-1} \tag{16}$$

Update state covariance:

$$P_{K+1} = P_{K+1/k} - G_{K+1}S_{K+1/k}{G_{K+1}}^T \tag{17}$$

Measurement residual:

$$V_{K+1} = Y_k - Y_{K+1} \tag{18}$$

Update state estimate:

$$X_{K+1} = \ X_{K+1/k} + G_{K+1}V_{K+1} \tag{19}$$

Where:

k- Discrete time,

$X_{K+1/k}$- State vector in the current state from the given previous state,

G_{K+1} − Kalman gain in discrete time,

$P_{K+1/k}$ −State covariance matrix of the current state from the given previous state,

$S_{K+1/k}$ - Measurement covariance matrix of the current state given the previous state,

X_{K+1} − Current estimated value by the Kalman filter.

From the updated state estimate, the fundamental components of the amplitude and phase angle using Eq. (20) and Eq. (21) are calculated.

$$\text{Magnitude (A)} = \sqrt{X_{(1)}^2 + X_{(2)}^2} \tag{20}$$

$$\omega t(or)\varphi = \arctan\left(\frac{X_{(1)}}{X_{(2)}}\right) \tag{21}$$

To examine the performance of the proposed Kalman algorithm in tracking the fundamental amplitude, phase and its robustness, a time-varying voltage signal with harmonics of the 1st, 3rd, 5th, 7th orders is taken, and Eq. (22) is created as a test signal.

$$Y(t) = 230\sin\omega t + 50\sin(3\omega t - 30^0) + 72\sin(5\omega t - 55^0) + 69\sin(7\omega t - 75^0) \tag{22}$$

Atypical distorted load voltage is shown in Fig. 2(a). The ideal phase angle is shown in Fig. 2(d), the PLL angle is shown Fig. 2(b) and the Kalman angle is shown in Fig. 2(c). The phase angle error value is depicted in Fig. 2(e) and Fig. 2(f) with the PLL and Kalman algorithms, respectively. Comparing Fig. 2(e) and Fig. 2(f) it is inferred that the Kalman algorithm produces a better phase angle with its negligible error.

Fig. 2(g) represents the amplitude error of the SRF-PLL and Kalman. Thus, the pictorial representation shows that the Kalman algorithm is superior when compared to the conventional algorithm.

Thus, the results obtained Fig. 2 make it possible to adopt this algorithm in a UPQC system.

IV. UPQC CONTROL METHOD

The main objective of a UPQC controller is to find the reference voltage and current. The proposed algorithm in the digital Kalman estimator estimates the fundamental component

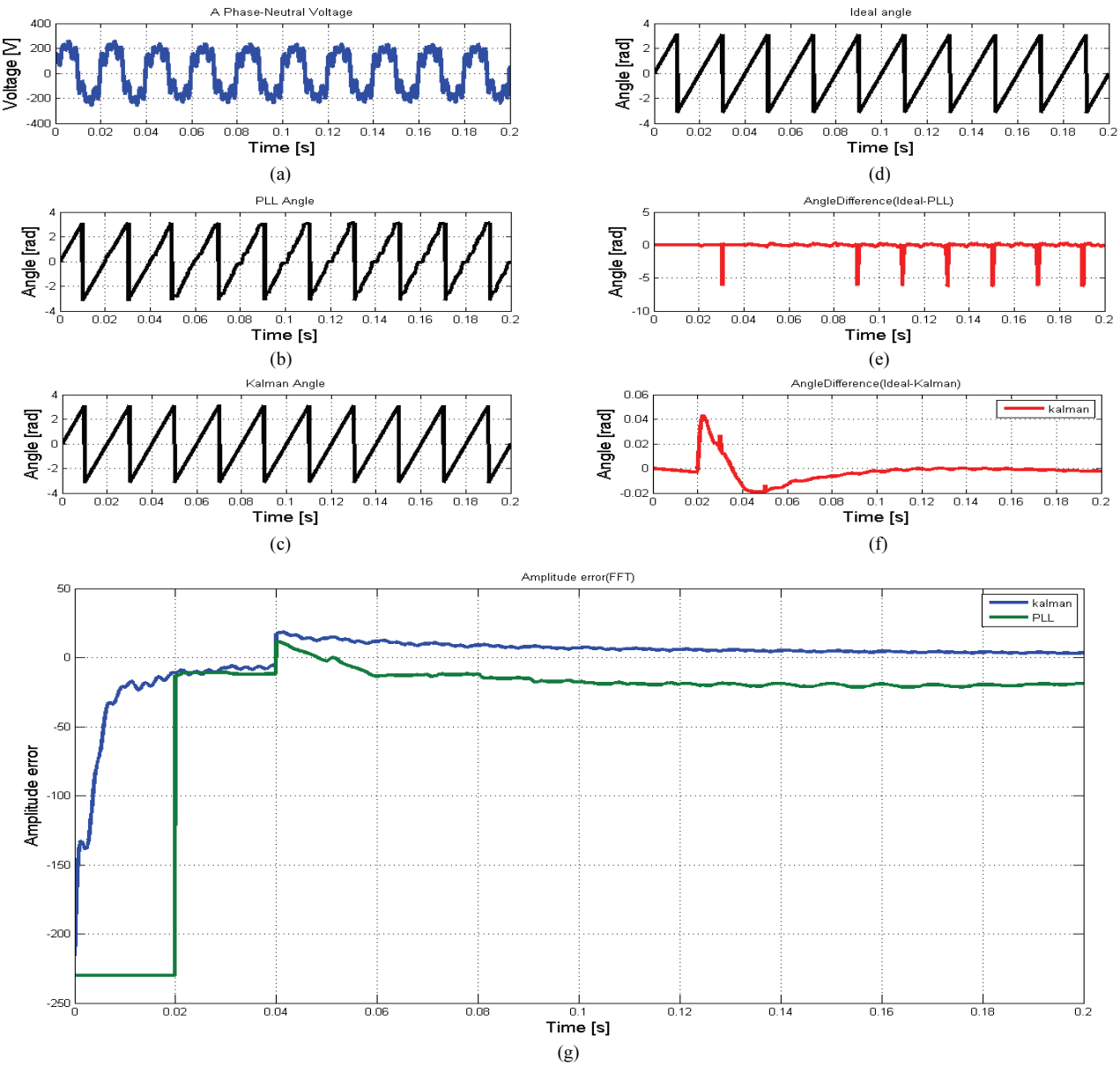

Fig. 2. Phase angle and amplitude estimation error with the PLL and Kalman techniques for the fundamental frequency.

of source voltage and load current. Using these fundamental components, the reference voltage and current are calculated. In order to find out the distortion of the load current and source voltages, the original distorted signal is subtracted from the reference signal.

A. Control Technique Used for Shunt Active Power Filter

The purpose of the shunt active filter is to compensate the harmonic and reactive components of load current, to regulate DC link voltage under normal, sag, swell and distorted conditions. The above factors are realized through the proposed control scheme as shown in Fig. 3(a). The measured load current which is given to the Kalman estimator brings out the fundamental component of the magnitude of current and phase angle for each phase using Eqns. (20) and (21). The DC link source current (I_{dc}) is found through a proportional-integrator (PI) controller to maintain the DC link voltage at its rated value. The active component of the source current is acquired by adding a DC link source current and a fundamental component. To find the reference sinusoidal current, the active component of the source current is multiplied by the unit amplitude sinusoidal signal which is obtained from the phase angle of a Kalman estimator. Thus, the required compensation current is obtained by subtracting the load current from the reference sinusoidal current.

B. Control Technique Used for Series Active Power Filter

As in series active filters, the sinusoidal rated voltage remains unchanged irrespective of voltage variations at the PCC. Fig. 3(b) shows the proposed series APF control

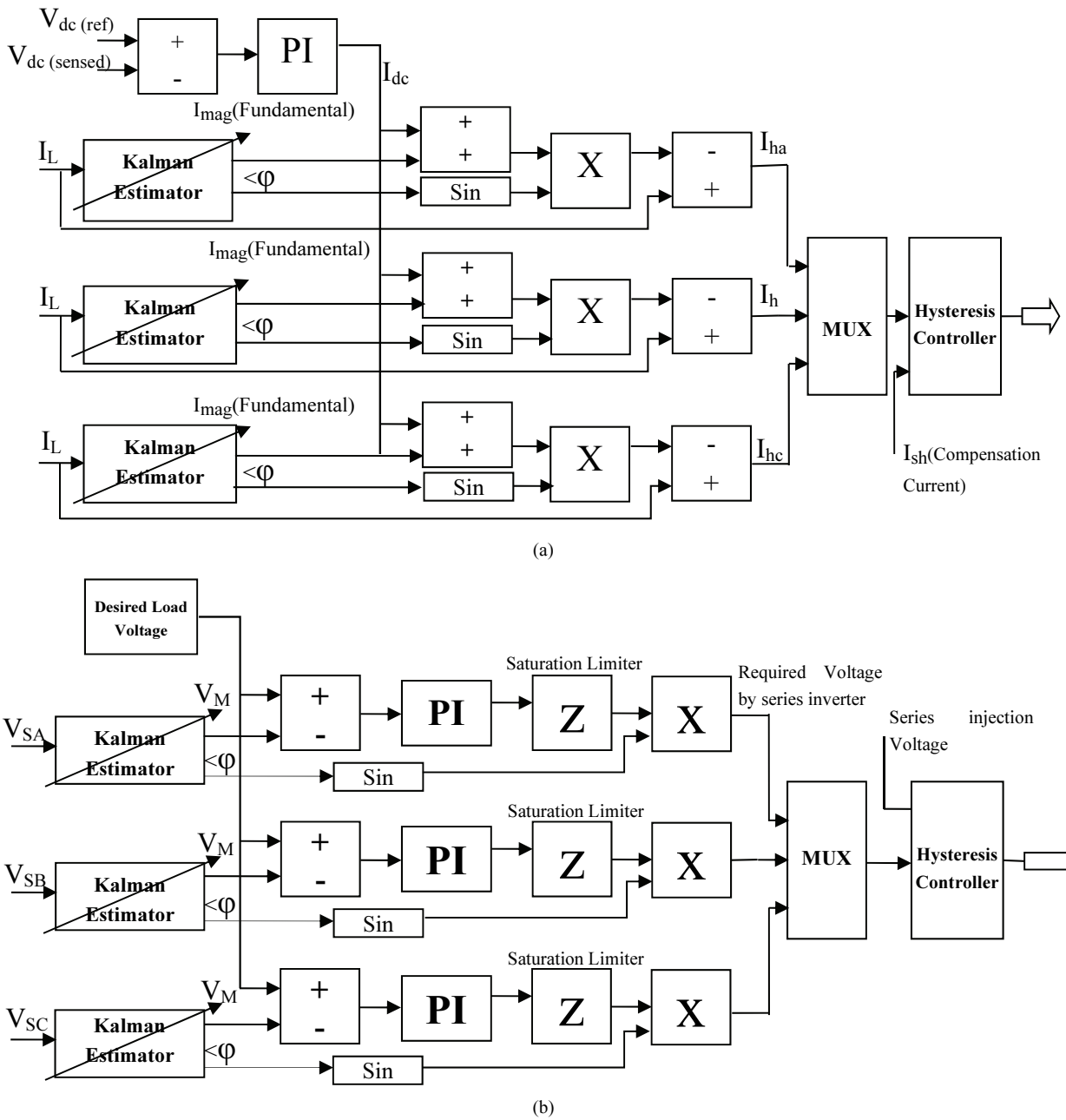

Fig. 3. Proposed APF control scheme: (a) functional block of the shunt APF strategy (b) functional block of the series APF strategy.

scheme. The Kalman estimator brings out the fundamental magnitude of the voltage and phase angle as presented in Eqns. (20) and (21). In order to obtain the required compensation voltage, the above fundamental voltage is subtracted from the desired load voltage, which is given to the PI controller. This compensated voltage is multiplied by the unit amplitude sinusoidal signal, which leads to the reference compensating sinusoidal voltage.

V. Simulation Results and Discussions

The simulation work done through MATLAB/Simulink incorporated a combination of a linear and three-phase rectifier loads with a different RL combination. The simulated parameters are given in Table I. In this analysis, the proposed Kalman based control algorithm for the UPQC is evaluated under balanced and distorted source voltage conditions.

Simulation results are obtained under the following conditions:

- Ideal voltage source
- Balanced and distorted voltage source
- Unbalanced voltage source
- Unbalanced and distorted voltage source

A test system is created with respect to the simulation parameters and source conditions.

TABLE I
SIMULATION PARAMETERS

	Parameters		*Value*
Source	Voltage	V_{Ph-Ph}	415V
	Frequency	F	50Hz
	Inductance	L_{sabc}	0.1mH
	Resistance	Resistance	1mΩ
Load	3-phase AC Line inductance	L_{Labc}	2mH
	3-phase DC Resistor	R_{dc}	10Ω
	3-phase DC Capacitance	C_1	100μF
	Linear Load	P+jQ	1000+j5000
dc Link	Voltage	V_{DC}	720V
	DC Capacitor	C_{dc}	1000 μF
Shunt APF	AC Line Inductance	Lc_{abc}	1mH
	Filter Resistor	R_{Cabc}	1mΩ
	Hysteresis Band	BW	$\pm 1e^{-6}$
Series APF	AC Line Inductance	L_{Tabc}	5mH
	Filter Resistor	R_{Tabc}	1mΩ
	Filter Capacitor	C_{Tabc}	10 μF
	Hysteresis Band	BW	$\pm 1e^{-6}$
	Three single phase series Transformer	S	3.1KVA

TABLE II
DETAILS OF VARIOUS SOURCE VOLTAGE CONDITIONS

Balance	V_a =338.84 sin(ωt) V_b =338.84 sin(ωt-120) V_c =338.84 sin(ωt+120)
Balance With Distorted	V_a=338.84sinωt+20sin(3ωt-29^0)+20sin(5ωt-40^0)+20sin(7ωt--57^0) V_b=338.84sin(ωt-120)+20sin(3ωt-149^0)+20sin(5ωt-160^0)+20 sin(7ωt-177^0) V_c=338.84sin(ωt+120)+20sin(3ωt+149^0)+20sin(5ωt+160^0)+20sin(7ωt+177^0)
Un Balance	V_a=255.26sinωt V_b=184.5sin(ωt-120) V_c=184.5sin(ωt+120)
Un Balance With Distorted	V_a=255.26sinωt+50 sin(3ωt-29^0)+ 20sin(5ωt-40^0)+20 sin(7ωt--57^0) V_b=467.4sin(ωt-120)+20sin(3ωt-149^0)+20sin(5ωt-160^0)+ 20 sin(7ωt-177^0) V_c=467.4sin(ωt+120)-20sin(3ωt+149^0)+20sin(5ωt+160^0)+ 20 sin(7ωt+177^0)

The following dynamic conditions are in corporate into the simulations:

- 0 sec to 0.15sec - balanced distorted voltage condition,
- 0.15 sec to 0.2 sec - normal condition,
- 0.2 sec to 0.25 sec - unbalance voltage sags with distorted condition,
- 0.3 sec to 0.35 sec - an unbalanced voltage swell with unequally distorted condition is imposed and the parallel occurrence of a 100 % variation of the load current disturbances is rapidly introduced between 0.27 sec and 0.35 sec.

A detailed analysis of the UPQC network can be evaluated at momentary condition under a sudden change in the source and load. Fig. 4 shows simulation results of the same.

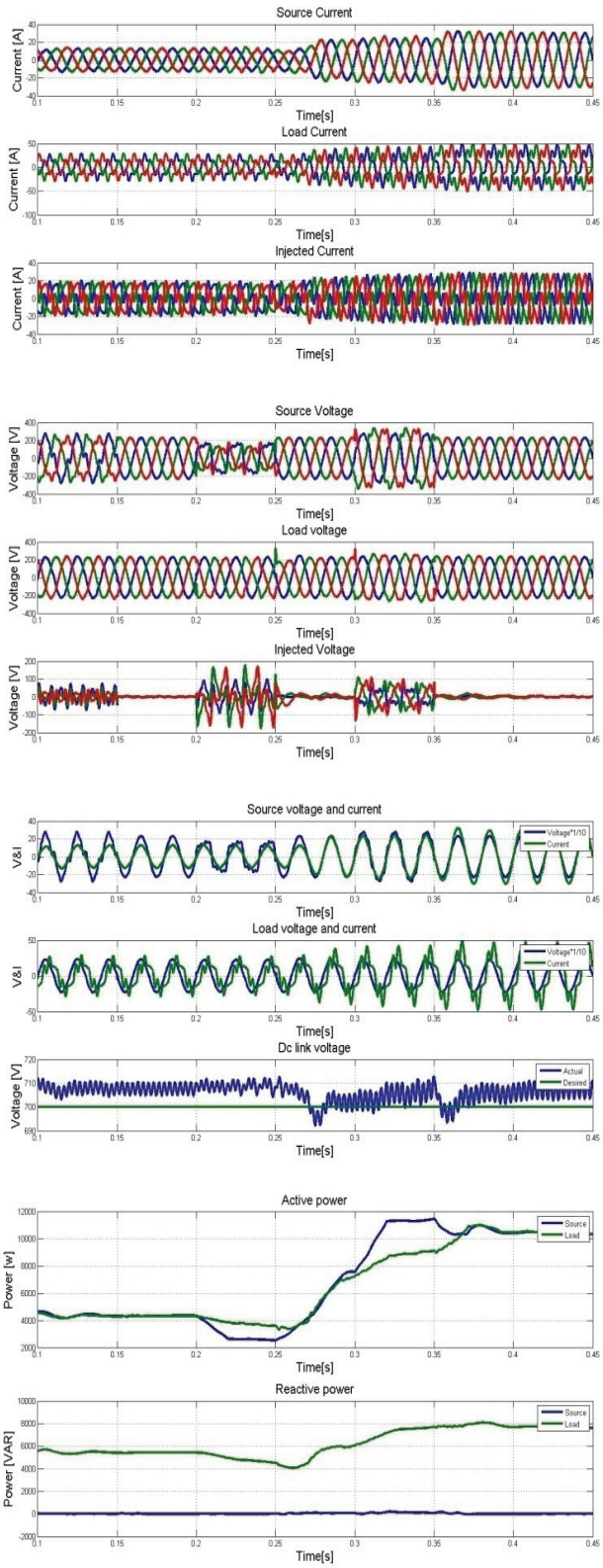

Fig. 4. Simulation results of the proposed UPQC control method.

The salient features of the proposed algorithm are as follows:

TABLE III
COMPARISON OF THE CONVENTIONAL AND THE PROPOSED UPQC CONTROL METHODS

Condition of PCC	Phases	Without UPQC		With UPQC			
				Conventional (PLL)		Proposed (Kalman)	
		I	V	I	V	I	V
Balanced	A	31.49	3.24	1.31	2.4	1.04	0.9
	B	32.28	6.65	1.42	2.2	1.06	0.9
	C	33.11	6.64	2.00	2.6	0.84	0.9
Balanced with distorted	A	30.61	27	4.04	10	3.33	2.3
	B	29.47	23	4.01	8.6	1.5	2.4
	C	33.39	15	3.05	6.4	2.72	2.3
Un balanced	A	28.08	4.94	1.52	4.2	1.32	0.7
	B	29.01	4.93	1.61	3.5	1.48	2.9
	C	37	4.94	1.59	3.8	1.56	3.8
Unbalanced with distorted	A	41.58	27.7	4.23	15.3	1.49	0.9
	B	31.6	23.0	4.85	12.5	1.23	1.0
	C	36.78	13.3	4.16	8.5	1.34	1.1

TABLE IV
COMPARISON OF THE DC-LINK VOLTAGE CONTROL PERFORMANCE OF A PI CONTROLLER WITH A SRF, A ROT CONTROLLER WITH A UVT AND A KALMAN FILTER

Time required for stabilization of DC-link voltage	PI controller with SRF[19]	ROT controller with UVT[20]	PI controller with Kalman filter
Initial stage	0.05 sec	0.015 sec	0.01 sec
150%load change	0.075 sec	0.05 sec	0.025sec
200%load change	0.075 sec	0.05 sec	0.02sec
sag Condition	0.12 sec	0.05 sec	<0.01sec
swell condition	0.11 sec	0.06 sec	<0.01sec

- ✓ Load voltage that is free from distortion.
- ✓ Reaches fundamental sinusoidal waveform.
- ✓ Balanced sinusoidal three phase load voltage.
- ✓ Magnitude of the source reactive power to achieve zero.

The above features are shown in a graphical representation in Fig. 4. Evaluating the dynamic conditions of a DC link capacitor with a PI controller, it has been observed that the voltage is constant and equal to the reference value ($V_{dc\text{-}ref}$ = 700 V).

It should also be noted that the DC voltage takes a time period of 0.02 sec before reaching a stable condition with a variation of 10V in its amplitude. Thus, through the visualization (in Fig. 4), it can be concluded that the proposed system is successfully operated. The simulated results are presented in Table III.

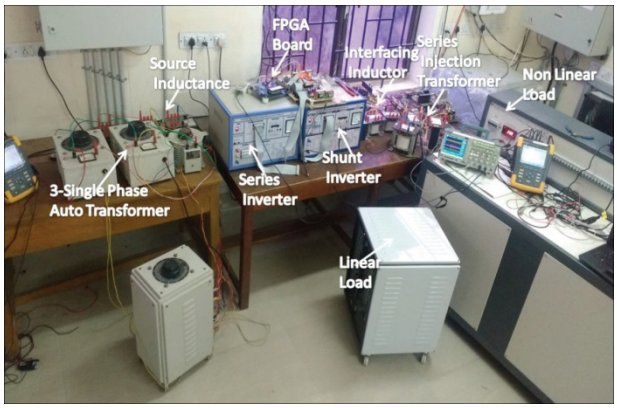

Fig. 5. Experimental set-up of UPQC.

TABLE V
EXPERIMENTAL PARAMETERS

Source	Supply voltage: 110 Vrms , 50 Hz Source Impedance: Rs = 0.047Ω and Ls = 120 μH/10A
UPQC	DC-link capacitors, Cdc =2200μF Reference dc-link voltage = 290 V Series filter, Lsr=2.5mH,Csr=15μF Shunt filter, Lsh = 5mH /5A Series transformer = 110/110 V (1:1 ratio), 500VA
Load	Linear: R = 27Ω and L = 50 mH Nonlinear R = 57Ω and L = 5 mH

VI. EXPERIMENTAL STUDY

An experimental setup is built to carry out tests under varied operating conditions to validate the newly presented control algorithm. A Spartan 3A DSPXC3SD1800 FPGA-based starter board is utilizing to send a train of switching pulses to a series and shunt inverter so that the envisaged control algorithm is realized. The FPGA board can operate up to a synchronous clock rate of 300 MHz and both of the inverters operate at a switching frequency of 10 kHz. A photograph of the experimental prototype is shown in Fig. 5. For emulating swell, sag, a harmonic and unbalanced distortion in the source voltage, a combination of three single phase transformers along with a variable inductor is employed. The experimental parameters of the system are listed in Table V. It is worth mentioning that in all of the results obtained through experimentation, the PCC and load voltages are indicated as line-to-phase voltages, while their counterpart series-injected voltages are expressed as phase voltages across a series transformer.

A. Performance Analysis of a UPQC at a Nonlinear Load under Balanced Source Conditions

Dynamic sag and swell conditions of the UPQC-connected system are depicted in Fig. 6. Initially the system is under steady state condition. For the first five cycles, a 9% voltage sag is introduced and for the next five cycles a 27% sag is introduced and finally an18% swell is induced for the next

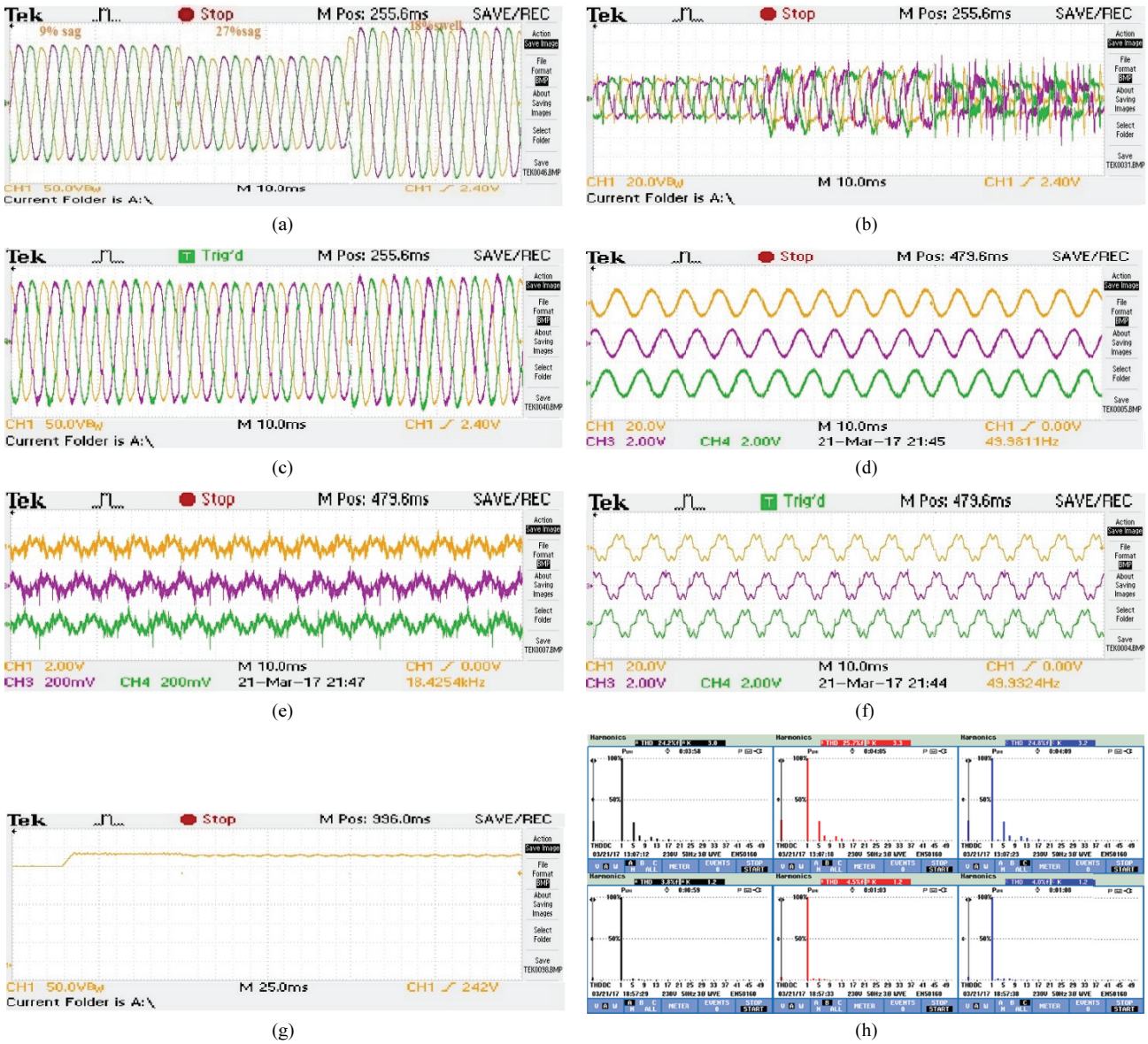

Fig. 6. Experimental results: transition from the steady state to balanced voltage sag and swell conditions (with a non-linear load).

five cycles. The required compensating voltages with respect to dynamic variations of the source voltage are shown in Fig. 6(b). The load voltage is kept constant irrespective variations of the source voltage, which is supported by a series compensator (DVR). This is depicted in Fig. 6(c). The PCC (point common coupling) is permanently connected across the rectifier load. As a result, the voltage and current at the PCC get distorted. In order to reduce the THD value to less than 5%, a shunt compensator is introduced. The sinusoidal source current, non-linear load current and compensator current are exhibited in the Fig. 6(d)-(f), which demonstrates the elimination of harmonic oscillation using DSTACOM. From Fig. 6(h) the harmonic spectra, the THD of the load currents and the source currents are shown, and numerically the THD is 25.1% on the load side and 3.7% on the source side.

B. Performance Analysis of UPQC at a Nonlinear Load under Unbalanced Source Conditions

An auto transformer, as shown in Fig. 5, is used to introduce unbalanced voltage sags and swells in the source voltage. From Fig. 7(a), at the t_1 instant, one phase voltage variations are introduced for five cycles, and at the t_2 instant, two phase voltage variations are induced for the next five cycles. Later, at the $t_3$instant, an unbalanced swell is introduced for the following cycles. Here the function of the series compensator is to inject the missing components in-phase with the respective phase voltages that are in the sag period and to injecting the out-phase with the phase voltage for swell periods as shown in the Fig. 7(a)-(b). The load voltage is also maintained at its rated value in this case, which is shown in Fig. 7(c). In addition, harmonics in the

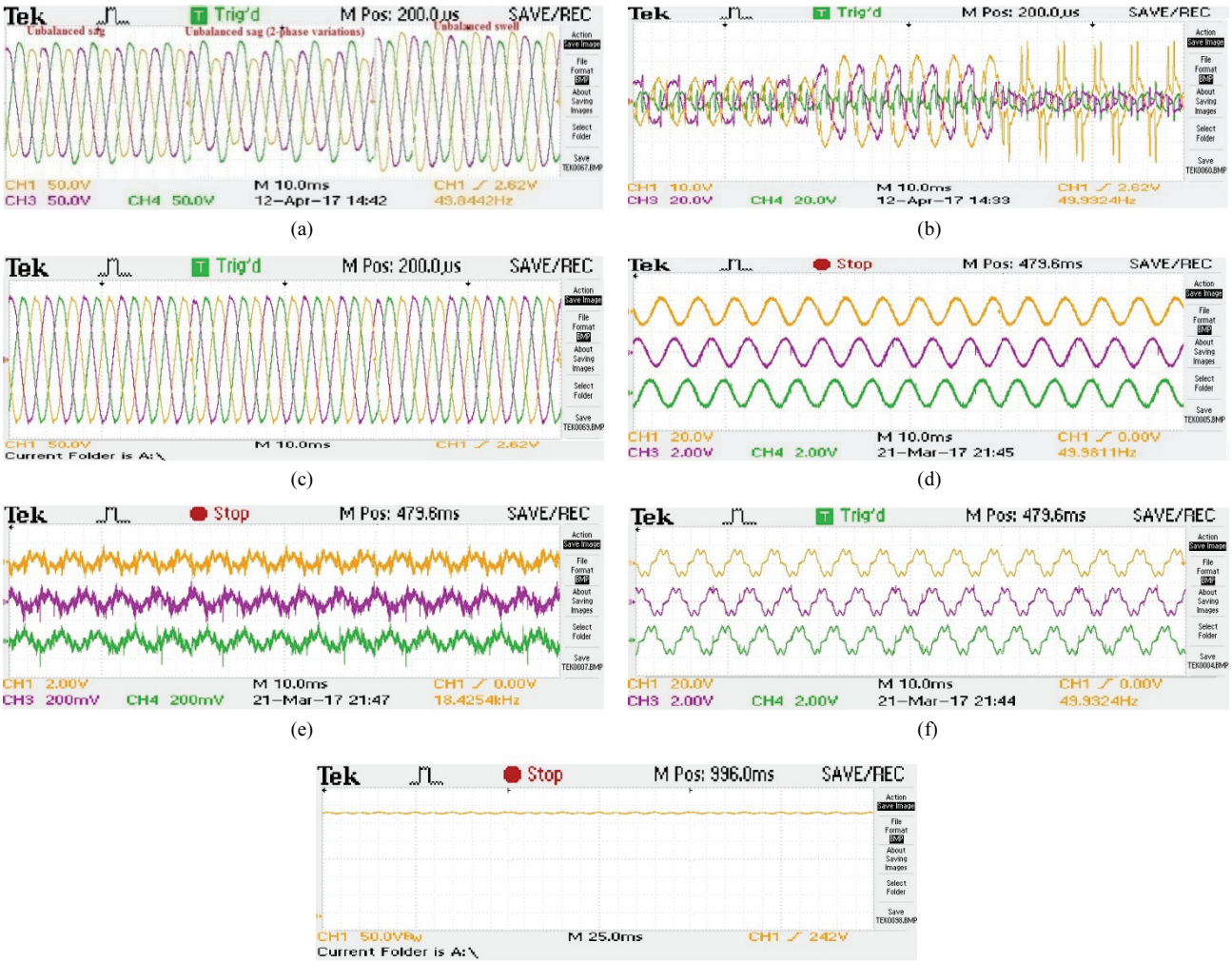

Fig. 7. Experimental Results: transition from the steady state to unbalanced voltage sag and swell conditions (with a non-linear load).

load sag and swell distorted condition (with a non-linear load) current are compensated by a shunt VSI. Thus, the DC-link voltage is maintained at its reference value so that the THD is less than 5% of the source current.

C. Performance Analysis of UPQC at Unbalanced Distorted Source Conditions

Source voltage is added to the fifth and seventh harmonic voltages where the sag and swell conditions are under unbalanced conditions, as shown in Fig. 8(a). 25 % of the THD load current is connected to the PCC. The series compensator helps in injecting the required voltage. It also helps in this operation. This is depicted in the Fig. 8(b). The enhanced load voltage profile is clearly observable from Fig. 8(c), where the THD is reduced to 3%. The shunt controller comes alive by simultaneously working and effectively compensating the load current harmonics by realizing sinusoidal source currents with a THD of 2.1%. As a result, in the above dynamic condition, the DC link voltage should be maintained at a constant value. The required value for this is shown in Fig. 8(g).

D. Dynamic Response of Current Harmonics Compensation under Load Changes

The dynamic load changes with linear and non-linear combinations, where the load combination is tested on the same system. At thet$_1$instant, a linear load acts, and at the t_2 instant, a non-linear load is added. Under this condition, the source current has to be sinusoidal and the DC link voltage variations should be less than 5 volts. Thus, through the visualization in Fig. 9, the source power factor will be improved from 0.94 to 0.98, which is near to a unity power factor.

At the outset, the source voltage is perturbed and its outcome is noticed. The results are then weighed. While doing so, it is obvious that the Kalman method has an edge over the others and yields better results than the PLL method, in terms of the phase angle (ωt) and the phase angle error, which can be easily noticed from Fig. 10(a)-(b). From the above proof, it is inferred that the Kalman method provides better results than the PLL.

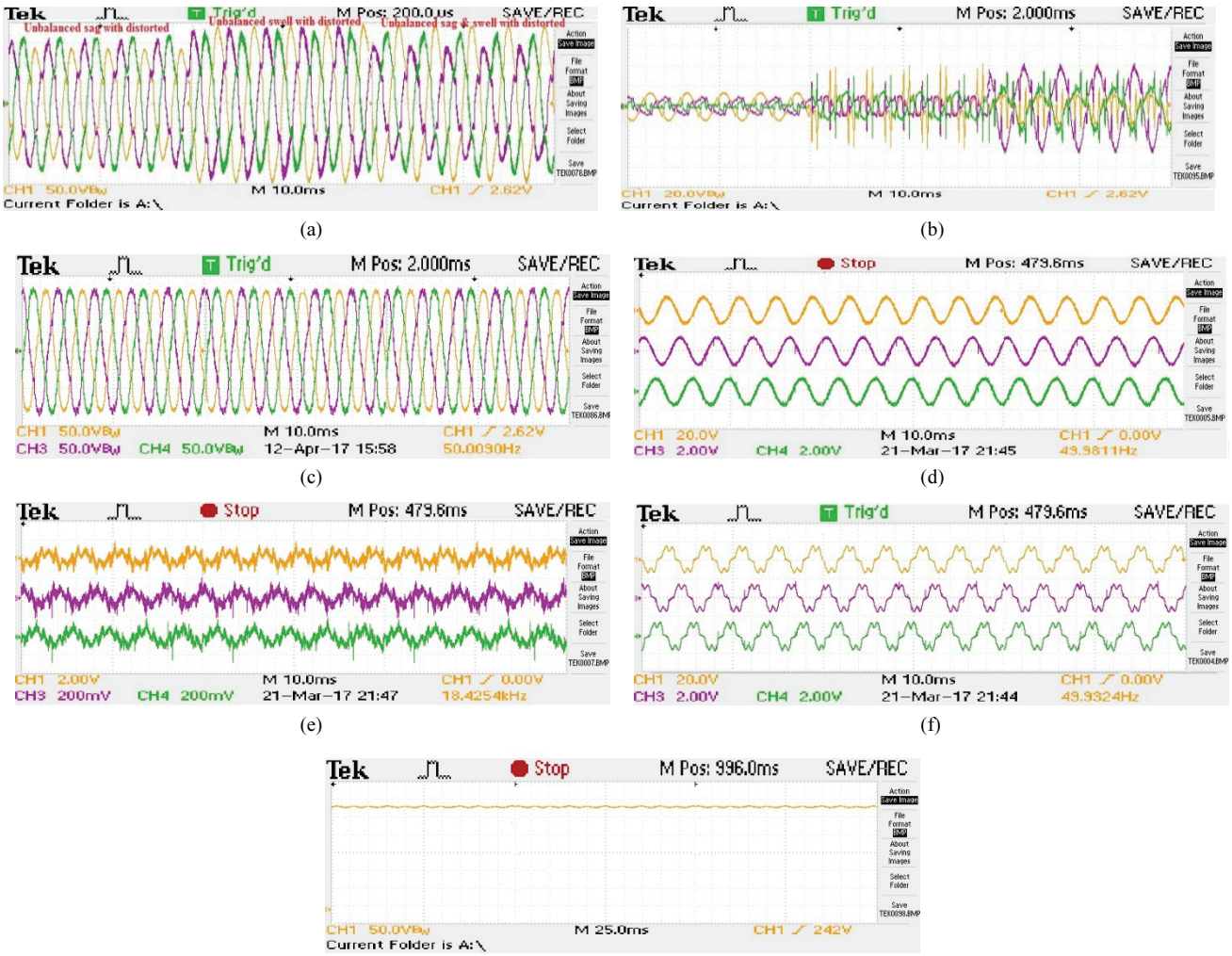

Fig. 8. Experimental results: transition from the steady state to unbalanced voltage distortions.

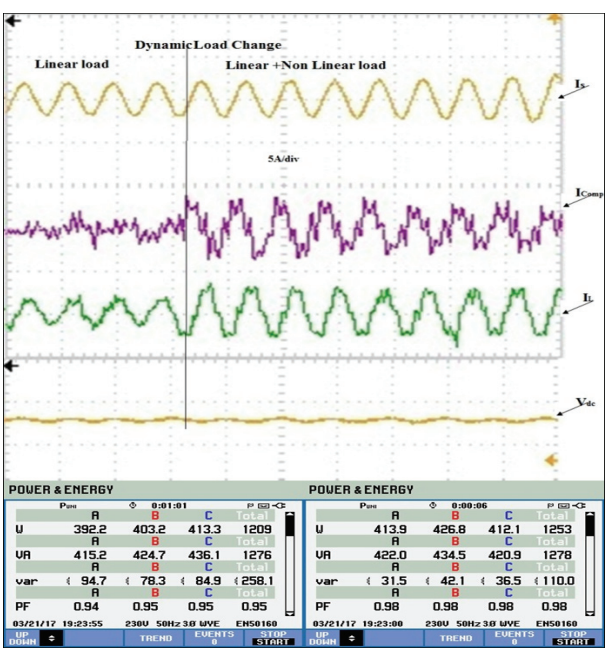

Fig. 9. Dynamic conditions of a UPQC.

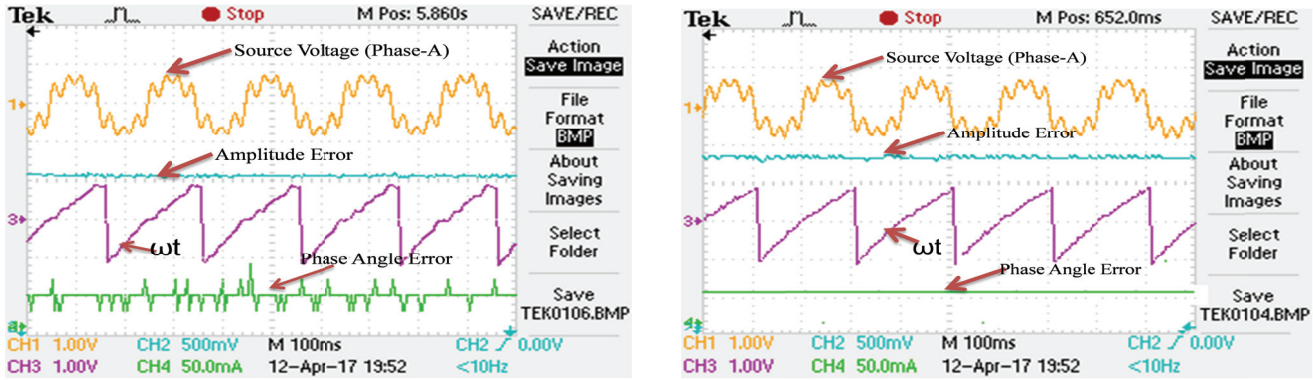

(a) (b)

Fig. 10. Experimental results: (a) PLL; (b) Kalman algorithm with distorted conditions.

TABLE VI
Simulation and Experimental Results at the PCC

Condition of PCC	Without UPQC		With UPQC							
			Proposed Kalman				Conventional PLL			
			Simulation Results		Experimental results		Simulation Results		Experimental results	
	I	V	I	V	I	V	I	V	I	V
Balanced with distorted	26.7	23	3.33	2.3	2.8	2.3	4.03	6.4	5.7	5.5
Unbalanced with distorted	27.5	24.4	1.44	1.1	3.0	2.0	4.85	8.5	6	7.8
Source side Power factor	0.88		~1		0.98-0.99		0.93		0.92	
Phase Angle error			~0 radians		~0 radians		5 radians		6radians	

VII. Conclusion

The article recommends that, for generating the fundamental component of the load current and source voltage, a digital Kalman control algorithm can be used, which can be acquired by a LS algorithm. It is shown that the phase angle and amplitude of an uneven distorted waveform can be determined precisely and very quickly by a Kalman filter.

In a distribution system, with the help of a UPQC, a modern control strategic method has been developed to generate the current and voltage references of series and shunt APFs.

A thorough evaluation of the proposed control strategy's performance is done by varying linear and non-linear RL loads. Simulation results illustrate that the envisaged control strategy has an edge over the SRF-PLL method. Through a FPGA-based UPQC implementation, which is found to be flexible and successful, the proposed algorithm can be validated. Thus, the Kalman control algorithm decreases the compensated THD source current from 27.5% to 1.44% in simulations and to 3% in experiments. In addition, the load THD voltage decreases from 24.4% to 1.1% and 2% for simulations and experiments, respectively. This algorithm also compensates voltage sags, voltage swells and reactive power. The source side power factor is also compensated from 0.88 to almost unity. The DC capacitor voltage sustains to its reference value in less than 0.01seconds under all operating conditions. The effectiveness of the proposed algorithm in both the steady and dynamic state conditions is verified via simulations and hardware tests.

In the long run, the proposed method will pave the way for researchers by enlightening them about the UPQC in the fields of renewable energy integration and smart grids.

Acknowledgment

The Authors Wish to Thank the Electrical and Electronics Engineering Department, Government College of Technology, Coimbatore, Tamilnadu, India, For Providing Us Financial Support Under TEQIP (Technical Education Quality Improvement Program) - Phase-II – sub module - Centre Of Excellence - Alternate Energy Research Lab.

References

[1] P. L. Jansen and R. D. Lorenz, "Transducerless position and velocity estimation in induction and salient AC machines," *IEEE Trans. Ind. Appl.*, Vol. 31, No. 2, pp. 240-247, Mar./Apr. 1995.

[2] G. T. Heydt, "Electric power quality: a tutorial introduction,"

IEEE Trans. Comput. Appl. Power, Vol. 11, No. 1, pp. 15-19, Jan. 1998.

[3] I. Hunter, "Power quality issues-a distribution company perspective," Power Eng. J., Vol. 15, No. 2, pp. 75-80, Apr. 2001.

[4] G. A, Ledwich, *Power Quality Enhancement Using Custom Power Devices*, London: Kluwer Academic Publishers, 2002.

[5] V. Khadkikar, "Enhancing electric power quality using UPQC: A comprehensive overview," *IEEE Trans. Power Electron*., Vol. 27, No. 5, pp. 2284-2297, May 2012.

[6] H. Fujita and H. Akagi, "The unified power quality conditioner: The integration of series and shunt-active filters," *IEEE Trans. Power Electron*., Vol. 13, No. 2, pp. 315-322, Mar. 1998.

[7] M. Basu, S. P. Das, and G. K. Dubey, "Comparative evaluation of two models of UPQC for suitable interface to enhance power quality," *Elect. Power Syst. Res*., Vol. 77, pp. 821-830, May 2007.

[8] P. Venkatesh Kumar, and R.Rajeswari, "Adaptive voltage detection controlled based single phase UPQC," *IEEE 2016 (ISCO'16) International Conference on Intelligent Systems and Control IEEE*, pp. 1-6, 2016.

[9] V. Soares, P. Verdelho, and G. D. Marques, "An instantaneous active and reactive current component method for active filters," *IEEE Trans. Power Electron.*, Vol. 15, No. 4, pp. 660-669, Jul. 2000.

[10] M. I. M. Montero, E. R. Cadaval, and F. B, Gonzalez, "Comparison of control strategies for shunt active power filters in three-phase four-wire systems," *IEEE Trans. Power Electron*., Vol. 22, No. 1, pp. 229-236, Jan. 2007.

[11] B. Singh and J. Solanki, "A comparison of control algorithms for DSTATCOM," *IEEE Trans. Ind. Electron.*, Vol. 56, No. 7, pp. 2738-2745, Apr. 2009.

[12] S. Charles and P. V. Kumar, "Modelling, simulation and implementation of optimization algorithm based shunt active filter for harmonics mitigation of nonlinear loads," *Aus. J. Elec. Electron Eng*, Vol, 9, No. 1, pp. 77-87, Nov. 2012.

[13] P. Kanjiya, V. Khadkikar, and H. H. Zeineldin, "A noniterative optimized algorithm for shunt active power filter under distorted and unbalanced supply voltages," *IEEE Trans. Ind. Electron.*, Vol. 60, No. 12, pp. 5376-5390, Dec. 2013.

[14] P. Salmeron, J. C. Montano, J. R. Vazquez, J. Prieto, and A. Valles, "Compensation in nonsinusoidal, unbalanced three-phase four-wire systems with active power line conditioner," *IEEE Trans. Power Del*., Vol. 19, No. 4, pp. 1968-1974, Oct. 2004.

[15] M. Kesler and E. Ozdemir, "Synchronous reference frame (SRF) based control method for UPQC under unbalanced and distorted load conditions," *IEEE Trans. Ind. Electron*., Vol. 58, No. 9, 3967-3975, Sep. 2011.

[16] N. Gupta, S. P. Singh, and R. C. Bansal, "A digital signal processor based performance evaluation of three-phase four wire shunt active filter for harmonic elimination, reactive power compensation and balancing of non-linear loads under non-ideal mains voltages," *Electric Power Component and Systems*, Vol. 40, No. 10, pp. 1119-1148, Jul. 2012.

[17] K. H. Kwan, Y. C. Chu, and P. Lam, "Model-based H∞ control of a unified power quality conditioner," *IEEE Trans. Ind. Electron*., Vol. 56, No. 7, 2493-2504, Jul. 2009.

[18] K. H. Kwan, Y. C. Chu, and P. Lam, "An output regulation-based unified power quality conditioner with Kalman filters," *IEEE Trans. Ind. Electron*., Vol. 59, No. 11, 4248-4262, Nov. 2012.

[19] J. M. Kanieski, R. Cardoso, H. Pinheiro, and H. A. Gründling "Kalman filter-based control system for power quality conditioning devices," *IEEE Trans. Ind. Electron*., Vol. 60, No. 11, 5214-5227, Nov. 2013.

[20] A. J. Viji and T. A. A. Victoire, "Enhanced PLL based SRF control method for UPQC with fault protection under unbalanced load conditions," *Int J. Electr Power Energy Syst*., Vol. 58, pp. 319-328, Jun. 2014.

[21] R. K. Patjoshi and K. K. Mahapatra, "Resistive optimization with enhanced PLL based nonlinear variable gain fuzzy hysteresis control strategy for unified power quality conditioner," *Int J Electr Power Energy Syst*, Vol. 83, pp. 352-363, 2016.

[22] C.-H. Huang, C.-H. Lee, K.-J. Shih, and Y.-J. Wang, "A robust technique for frequency estimation of distorted signals in power systems," *IEEE Trans. Instrum. Meas.,* Vol. 59, No. 8, pp. 2026-2036, Aug. 2010.

[23] K. W. Louie, P. Wilson, R. Mazur, K. Kent, H. W. Dommel, and J. R. Marti, "Power system harmonic analysis in the frequency domain," *Electrical and Computer Engineering, 2007. CCECE 2007. Canadian Conference on*, pp.1421-1424, 2007.

[24] H. Ma and A. A. Girgis, "Identification and tracking of harmonic sources in a power system using a Kalman filter," IEEE Trans. Power Del., Vol. 11, No. 3, pp. 1659-1665, Jul. 1996.

[25] M. S. Sachdev and M. M. Giray, "A least square technique for determining power system frequency," *IEEE Trans. Power App. Syst.*, Vol. PAS-104, No. 2, pp. 437-443, Feb. 1985.

[26] R. A. Wiltshire, G. Ledwich, and P. O'Shea, "A Kalman filtering approach to rapidly detecting modal changes in power systems," *IEEE Trans. Power Syst.*, Vol. 22, No. 4, pp. 1698-1706, Nov. 2007.

[27] V. M. Moreno and J. Barros, "Application of Kalman filtering for continuous real-time tracking of power system harmonics," *IEE Proceedings – Generation, Transmission and Distribution*, Vol. 144, No. 1, Jan. 1997.

[28] G. G. Rigatos, "A derivative free Kalman filtering approach to state estimation based control of nonlinear systems," *IEEE Trans. Ind. Electron.*, Vol. 59, No. 10, pp. 3987-3997, Oct. 2012.

Venkatesh Kumar received his BE degree in Electrical and Electronics Engineering and his ME in Power Systems from the Anna University of Technology, Tamil Nadu, India, in 2004 and 2010, respectively. He is presently working as an Assistant Professor in the Department of Electrical Engineering, Karunya University, Coimbatore and Tamilnadu, India. His current research interests include optimization techniques, power electronics applications to power systems and power quality.

Rajeswari Ramachandran received her B.E degree in Electrical and Electronics Engineering and her M.E. degree in Power Systems Engineering from Madurai Kamaraj University, Madurai, India, in 1995 and1997, respectively. She received her Ph.D. degree from Anna University, Chennai, India, in 2009. She is presently working as an Associate Professor in the Department of Electrical Engineering, Government College of Technology, Coimbatore and Tamilnadu, India. She has published a number of papers in the area of soft computing, power system operation and control and smart grid. She is a life Member of ISTE (Indian Society for Technical Education).